Biophysical *Journal*
Biophysical Letter

Biophysical Society

Ryanodine Receptor Open Times Are Determined in the Closed State

Michael Fill[1] and Dirk Gillespie[1,*]
[1]Department of Physiology and Biophysics, Rush University Medical Center, Chicago, Illinois

ABSTRACT The ryanodine receptor (RyR) ion channel releases Ca^{2+} from intracellular stores by conducting Ca^{2+} but also by recruiting neighboring RyRs to open, as RyRs are activated by micromolar levels of cytosolic Ca^{2+}. Using long single-RyR recordings of the cardiac isoform (RyR2), we conclude that Ca^{2+} binding to the cytosolic face of RyR while the channel is closed determines the distribution of open times. This mechanism explains previous findings that RyR is not activated by its own fluxed Ca^{2+}. Our measurements also bolster previous findings that luminal [Ca^{2+}] can affect both the cytosolic activation and inactivation sites and that RyR has different gating modes for the same ionic conditions.

In cardiac myocytes, ryanodine receptors (RyRs) release Ca^{2+} from the sarcoplasmic reticulum to initiate muscle contraction. Because RyRs open in response to micromolar [Ca^{2+}], the efflux of Ca^{2+} through one RyR is amplified by the recruitment of nearby RyRs. Although this inter-RyR Ca^{2+}-induced Ca^{2+} release is largely understood, one open question is the extent to which the Ca^{2+} released by a RyR acts on itself (feedthrough activation).

Previous studies showed that RyR generally does not react to its own fluxed Ca^{2+}, with feedthrough activation only for superphysiological currents (>3 pA, compared to ~0.4 pA under physiological conditions) (1,2), or for RyRs that are hypersensitive to Ca^{2+} by the application of caffeine (2) or ATP (3), or in the absence of cytosolic Mg^{2+} (3,4). ATP and Mg^{2+} potently modulate RyR Ca^{2+} sensitivity and are present at high concentrations in cells. Therefore, including these substances is vital when evaluating the physiological role of feedthrough activation. Our experiments with both ATP and Mg^{2+} at physiological cytosolic levels show that RyR does not see its own fluxed Ca^{2+}; the open probability (P_o) (Fig. 1 *A*) is independent of Ca^{2+} flux <1 pA (Fig. 1 *B*).

RyR not reacting to its own fluxed Ca^{2+} is difficult to reconcile with other data, namely that RyR open time increases with cytosolic [Ca^{2+}] (1,2,5); mean open time (MOT) is shown in Fig. S5. Open channels are thought to close randomly. In that case, open times are defined while the channel is open. However, to be sensitive to cytosolic [Ca^{2+}], the cytosolic Ca^{2+} binding sites would have to be accessible to Ca^{2+} during the open state and exposed to the fluxed Ca^{2+}, which can raise Ca^{2+} concentration on the cytosolic face to >15 μM for physiological currents (6) and >50 μM in our experiments (Fig. S9). These

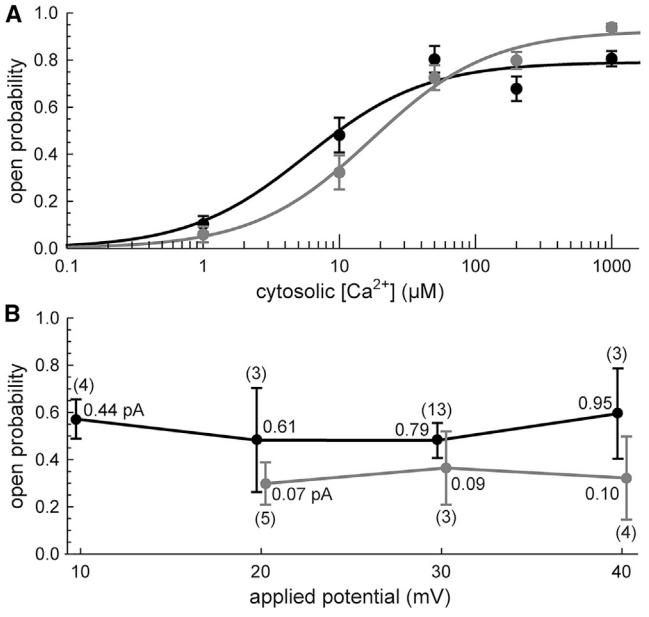

FIGURE 1 (*A*) P_o versus cytosolic [Ca^{2+}] for high (*black*) and low (*gray*) luminal Ca^{2+}. The lines are binding curves. (*B*) P_o versus applied voltage for high (*black*) and low (*gray*) luminal Ca^{2+}. Parentheses: number of recordings. Also listed are calculated Ca^{2+} currents. Cytosolic [Ca^{2+}] is 10 μM. Other [Ca^{2+}] are also independent of potential (data not shown). Details of the P_o analysis, binding curves, and Ca^{2+} currents are in the Supporting Materials and Methods.

Submitted June 28, 2018, and accepted for publication August 23, 2018.
*Correspondence: dirk_gillespie@rush.edu
Editor: Eric Sobie.
https://doi.org/10.1016/j.bpj.2018.08.025

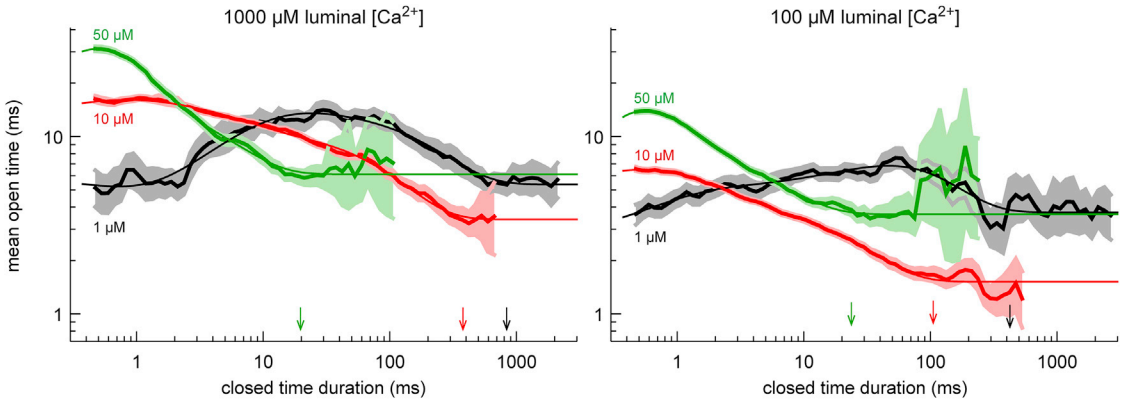

FIGURE 2 MOT versus duration of the previous closed event for 1, 10, and 50 μM cytosolic [Ca^{2+}] and for high (*left*) and low (*right*) luminal [Ca^{2+}]. The thick lines are the mean times of the data, and the shaded areas are the 95% confidence intervals (see Supporting Materials and Methods). The thin lines are fits of a sum of three exponentials, and the arrows indicate when these fits approximately reach steady state (i.e., $4\tau_3$, as defined in Fig. 3). Fig. S10 *A* shows the same for 200 and 1000 μM. Fig. S10 *B* shows mean closed time versus open duration. To see this figure in color, go online.

are substantially larger than needed to activate RyR (Fig. 1 *A*), leading to feedthrough activation.

Here, we test a hypothesis that explains how RyR open times can depend on cytosolic [Ca^{2+}] without having feedthrough activation: RyR open-time distributions are determined in the closed state, before the channel opens.

We do this by analyzing single-RyR2 recordings taken under conditions with high (1000 μM) and low (100 μM) luminal Ca^{2+} and with 1, 10, 50, 200, and 1000 μM cytosolic Ca^{2+}. For each condition, we recorded 8–20 channels for a total time of 13–75 min. (Further details are in the Supporting Materials and Methods; Tables S1 and S2.) This was done to ensure that we understand RyR behavior with cell-like cytosolic Ca^{2+}, Mg^{2+}, and ATP levels, but also because

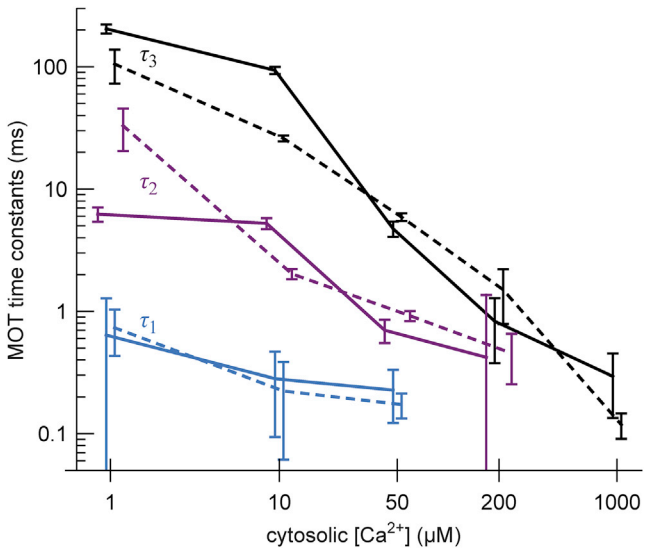

FIGURE 3 The time constants from the exponential fits in Fig. 2 and Fig. S10 *A* as a function of cytosolic [Ca^{2+}] for both high (*solid lines*) and low (*dashed lines*) luminal [Ca^{2+}]. To see this figure in color, go online.

there is variability between channels under identical conditions and within recordings. This variability is ubiquitous (Figs. S4 and S5), but subgroups of channels have identical open- and closed-time distributions, indicating a small number of gating modes for the same ionic condition (Fig. S6), a property that has been previously reported (7–10). Importantly, however, all our analysis is largely independent of this variability, shown in the figures with 95% confidence intervals (see Supporting Material).

We include data with both high and low luminal Ca^{2+} because each is known to affect the channel differently (11–14). RyR exposed to high luminal Ca^{2+} is more responsive to cytosolic Ca^{2+} (Fig. 1 *A*) and is also subject to inactivation at cytosolic [Ca^{2+}] $\geq$200 μM (Fig. S7), whereas at low luminal Ca^{2+} it is not; the high luminal Ca^{2+} case has a marked drop in MOT between 50 and 200 μM that the low luminal Ca^{2+} case does not (Figs. S5 and S8). We will show that at both high and low luminal Ca^{2+}, the open-time distributions are determined in the closed state.

To start the analysis, we plot MOT versus closed-time duration in Figs. 2 and S10 *A*. This shows how open time correlates to the length of the previous closing. (Fig. S13 shows this in a different way.) The curves are not identical, so it is not merely the length of a closing that determines open time. However, the curves overlap significantly when the closures are longer than ~3 ms, and this overlapping is consistent with our hypothesis that open-time distributions are determined in the closed state. We see from Fig. 2 that for each cytosolic [Ca^{2+}], a final MOT is reached; for long enough closures, each curve becomes a constant. Moreover, the higher the cytosolic [Ca^{2+}], the less time it takes to reach this steady state. Based on this, we hypothesize that there is an underlying Ca^{2+}-dependent process that determines channel open-time distributions (and therefore MOT) and that this process is faster at higher cytosolic [Ca^{2+}].

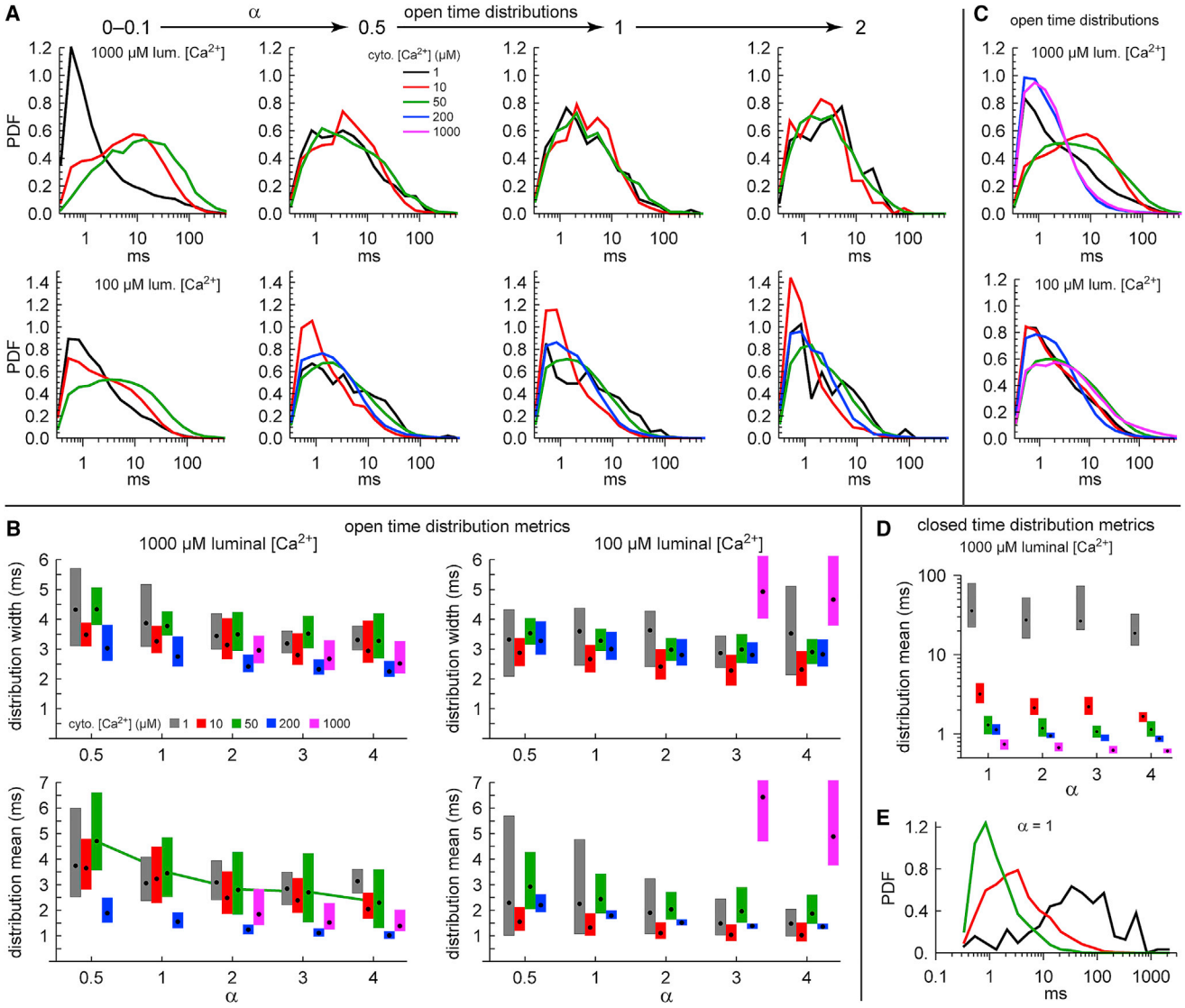

FIGURE 4 (*A*) The probability distribution functions (PDFs) of the open times for different scaled times α. When a specific α is listed, all events with closed times t with $0.9\alpha\tau_3 \leq t < 1.1\alpha\tau_3$ are chosen and the distribution of the subsequent open times is shown. Top row, high luminal Ca^{2+}; bottom row, low. (*B*) Metrics of the smoothed histograms described in the Supporting Materials and Methods, specifically the standard deviations (*top row*) and means (*bottom row*). (*C*) Open-time PDFs for all recorded openings are shown. (*D*) Distribution means are shown like in (*B*), but for closed-time distributions rather than open-time distributions. (*E*) PDFs are shown as in (*A*), but for closed-time distributions. To see this figure in color, go online.

To identify this underlying process, we fit the curves in Figs. 2 and S10 *A* (*thin lines*) with a sum of up to three exponentials (see Supporting Materials and Methods). Fig. 3 shows the cytosolic $[Ca^{2+}]$ dependence of these time constants.

If the time constants are from a single process, then the largest one (τ_3) defines the timescale it takes to reach steady state. Moreover, if this process defines RyR open-time distributions during the closed state, then the open-time distributions for each cytosolic $[Ca^{2+}]$ should be identical if the closed-time duration t is scaled by the τ_3 for each $[Ca^{2+}]$; i.e., it is not the absolute closed times that determine the open-time distributions, but rather the fraction of time α through the process ($\alpha = t/\tau_3$ and steady state is reached for $\alpha > \sim 4$ (*arrows* in Fig. 2)). We show this in Fig. 4.

Our goal is to show that the open-time distributions are identical for all cytosolic $[Ca^{2+}]$ after a sufficient amount of scaled time (α) has passed. We do this in several ways (with details described below): in Fig. 4 *A*, we show that the distributions look the same; in Fig. 4 *B*, we quantify distribution similarity using two metrics; in Fig. 4, *C*–*E*, we show negative controls; in Fig. S12, we show that the open-time distributions across cytosolic $[Ca^{2+}]$ are highly correlated.

Fig. 4 *A* shows how the open-time distributions change with α. The top row shows it for high luminal Ca^{2+}, the

bottom for low. Early in the process ($0 < \alpha < 0.1$), the distributions are very different from each other but quickly become the same as α increases. Fig. 4 *B* shows metrics of the distributions with 95% confidence intervals (see Supporting Materials and Methods); the top row shows the widths of the distributions (standard deviations), the bottom row the means. The purpose of these metrics is to quantify the similarity between the distributions, which are shown in Figs. S1 and S2.

The distributions in Fig. 4 *A* and the metrics in Fig. 4 *B* are highly similar, with a few exceptions.

First, at high luminal Ca^{2+}, the distribution means for 200 μM cytosolic Ca^{2+} are below those of the lower concentrations (*blue boxes* for all α in the *lower left panel* of Fig. 4 *B*). This is also true to a lesser extent for 1000 μM cytosolic Ca^{2+} (*magenta boxes*), whose metrics only appear for $\alpha \geq 2$ because its τ_3 is less than the shortest reliably measurable event time. We suspect that the reason for this is that at these high cytosolic Ca^{2+} concentrations, the Ca^{2+} is binding not only to the activation site of RyR but also to its inactivation site, which decreases MOT (Figs. S5 and S8). If this is the case, then the open-time distributions should be different. However, these distributions are still determined in the closed state, in line with our hypothesis.

Second, at low luminal Ca^{2+}, the distributions for 10 μM cytosolic Ca^{2+} (Fig. 4 *A*, *bottom row*, *red lines*) appear shifted to shorter open times. This is reflected in the distribution means (Fig. 2; *red boxes* in the *lower right panel* of Fig. 4 *B*), but here, the confidence intervals are very close to the distribution means for the other cytosolic [Ca^{2+}]; they are all within a fraction of a millisecond of each other. This case is different from the case above (high luminal and 200 μM cytosolic Ca^{2+}) in which the confidence intervals are far from overlapping with other data intervals. Therefore, we believe that this is more a reflection of the variability among channels than a fundamental difference in the distribution shapes. Moreover, if it were significantly different, then this 10 μM cytosolic Ca^{2+} data point would be qualitatively different from surrounding data points at both lower (1 μM) and higher (50 and 200 μM) cytosolic [Ca^{2+}].

Lastly, at low luminal Ca^{2+}, the distribution for 1000 μM cytosolic Ca^{2+} is far different from all other open-time distributions (*magenta boxes* in the *right panels* of Fig. 4 *B*). Both its mean and its width are much larger, which can also be seen in Fig. S10 *A* (*right panel*). This is not due to inactivation; mean closed time is shorter than for smaller cytosolic [Ca^{2+}], whereas MOT is longer (Fig. S5). In fact, its P_o is almost 1 (Fig. 1 *A*). At this point, it is not clear why this data point is so qualitatively different from all the others.

Except for this one outlier and when inactivation is present, we have now shown that open-time distributions of RyR are identical as long as sufficient time has passed in the closed state to be partly through a cytosolic Ca^{2+}-dependent process. This similarity between the open-time distributions is not because the distributions are the same to begin with; early in the process, the distributions are quite different (Fig. 4 *A*, *first column*) and gating may be stochastic (Fig. S13), and the open-time distributions for all the data (i.e., for all opening events) are also very different (Fig. 4 *C*). Moreover, the similarity is not because the distributions do not change with α; their means change (Fig. 4 *B*, *green line*). Lastly, to show a counterexample in which distributions do not cluster, we consider closed- (rather than open-) time distributions and their time constants (Figs. S10 *B* and S11). Applying the same analysis, we find qualitatively different distributions (Fig. 4, *D* and *E*). The point of this is to show that the similarity of the open-time distributions is not expected and to show that closed-time distributions do not seem to be determined during the open state.

Finally, in Fig. S12, we show the Pearson correlation between open-time distributions for all pairs of cytosolic [Ca^{2+}]. These high correlations, when combined with the analysis in Fig. 4 *B*, indicate each pair is the same (except cases noted above). Fig. S12 also shows that ~30% through the process is sufficient to reach identical distributions.

We next focus on the nature of the cytosolic Ca^{2+}-dependent process. Because RyR is activated by cytosolic Ca^{2+}, we hypothesized that this process is Ca^{2+} binding to the activation site on the cytosolic face. A binding process has the necessary characteristics: it is [Ca^{2+}] dependent and requires time to complete, which for simple models occurs through multiple, well-defined time constants. We first tried the simplest model, namely four independent binding sites, one on each of the four identical subunits of RyR. This has one time constant but failed to reproduce the [Ca^{2+}] dependence of the τ_3 (data not shown). Next, we considered a model in which RyR can bind 0–3 Ca^{2+} ions (assuming three Ca^{2+} bound to any of the four subunits is enough to activate the channel) with on and off rates depending on how many are bound. This model describes the Ca^{2+} dependence (both cytosolic and luminal) of all three time constants (Fig. S3). (Details of the Ca^{2+} binding analysis are given in the Supporting Material.)

The model also provides an explanation of how high and low luminal Ca^{2+} differ in the binding of Ca^{2+} during the closed state. Specifically, we find significant overlap between the on and off rates that reproduce the measured time constants, indicating similarities in some Ca^{2+} binding steps. But, we find that the binding of the first Ca^{2+} is stabilized at low luminal Ca^{2+}; the smaller time constants with low luminal Ca^{2+} come from preventing unbinding of the first Ca^{2+}, with the other parameters unchanged (Fig. S3 *C*).

This very simple Ca^{2+} binding model provides a reasonable explanation of our data, but our analysis is by no means exhaustive; other Ca^{2+} binding models may explain the data. However, because the overarching goal of this study is to show that RyR open times are determined in the closed state, we limit our analysis to providing one possible explanation of what the cytosolic [Ca^{2+}]-dependent process is that determines RyR open-time distributions.

The implications of our findings are far-ranging, both for RyR and ion channels in general.

With respect to RyR regulation by cytosolic Ca^{2+}, influencing open time by what occurs during the closed state is probably the simplest way to keep a Ca^{2+}-conducting, Ca^{2+}-sensitive channel from activating itself. If RyR were activated by its own fluxed Ca^{2+}, then some other mechanism would likely be necessary to control the closing of RyRs (e.g., some form of inactivation) lest all the RyRs in a cluster open (via inter-RyR Ca^{2+}-induced Ca^{2+} release) and stay open (via feedthrough activation) until sarcoplasmic reticulum Ca^{2+} is depleted. Moreover, cytosolic Ca^{2+} binding in the closed state is probably the only way for RyR to be sensitive to 1 μM Ca^{2+}. If RyR sensed cytosolic [Ca^{2+}] in the open state, the sensor would have to have extraordinarily fine sensitivity, distinguishing, for example, 50 μM from 51 μM (Fig. S9).

In this picture, Ca^{2+} released during an opening diffuses away and does not appreciably increase the background cytosolic [Ca^{2+}] seen by the RyR in the closed state. If this does not occur (e.g., in the tight geometry of the subsarcolemmal space), then the fluxed Ca^{2+} can reactivate RyR. Although more study is needed, we suspect that this is what occurs when we and other groups found feedthrough activation with Ca^{2+} fluxes ~10 times larger than physiological (1,2). Similarly, with caffeine, with ATP, or without cytosolic Mg^{2+}, the activation site is more sensitive to Ca^{2+} and MOT is increased, and therefore residual Ca^{2+} is more likely to trigger a new opening.

Our analysis also has implications about RyR regulation by luminal Ca^{2+}. It is already known that luminal Ca^{2+} affects RyR gating (11–14), although this is phenomenon is not universal (e.g., the Ca^{2+} sensitivity shift in Fig. 1 *A* is not present in mouse RyR2 or with the addition of exogenous CSQ (11)) and more studies are necessary. Our study provides evidence that luminal Ca^{2+} can alter function of both the cytosolic activation and inactivation sites. With respect to the inactivation site, low luminal [Ca^{2+}] seems to inhibit inactivation by preventing a drop in open times at high cytosolic [Ca^{2+}] (Figs. S5 and S8). With respect to the activation site, the different time constants for high and low luminal Ca^{2+} in Fig. 3 are direct evidence that the luminal side changes the properties of the cytosolic site. Specifically, the shorter time constants with low luminal [Ca^{2+}] indicate a faster setting of open times compared to high luminal [Ca^{2+}], especially at low cytosolic [Ca^{2+}]. Moreover, our modeling suggests that the affinity of the cytosolic Ca^{2+} binding site varies with luminal [Ca^{2+}] (and probably mainly the affinity for the first Ca^{2+}). Possible explanations include the occupancy state of the luminal Ca^{2+} binding site or a change in a luminal regulatory protein (e.g., unbinding) altering the cytosolic activation site architecture (11–14).

Our results also have implications for understanding ion channels in general, not just RyR. For example, our work shows that channel gating is not always a random occurrence. For RyR, we showed that there is memory between the closed and open states through how much Ca^{2+} is bound during the closed state; if the binding process is >30% completed (Fig. S12), then the open-time distributions are the same. At shorter closed times, however, the openings do seem to be more stochastic (Fig. S13).

Overall, our analysis indicates that this memory is vital to physiological RyR2 function so it can sense micromolar cytosolic [Ca^{2+}] and still mediate a large Ca^{2+} flux.

SUPPORTING MATERIAL

Supporting Materials and Methods, 13 figures, and two tables are available at http://www.biophysj.org/biophysj/supplemental/S0006-3495(18)30979-2.

AUTHOR CONTRIBUTIONS

The hypothesis was conceived by D.G. during discussions with M.F. M.F. provided the experimental data and contributed to the analyses and writing. D.G. conceived and performed the analyses and wrote the manuscript.

ACKNOWLEDGMENTS

We thank Prof. Lothar Blatter for his useful comments on the manuscript.

Research reported in this publication was supported by the National Institute of Arthritis and Musculoskeletal and Skin Diseases of the National Institutes of Health under award number R01AR054098.

SUPPORTING CITATIONS

References (15–24) appear in the Supporting Material.

REFERENCES

1. Liu, Y., M. Porta, …, M. Fill. 2010. Flux regulation of cardiac ryanodine receptor channels. *J. Gen. Physiol.* 135:15–27.
2. Xu, L., and G. Meissner. 1998. Regulation of cardiac muscle Ca^{2+} release channel by sarcoplasmic reticulum lumenal Ca^{2+}. *Biophys. J.* 75:2302–2312.
3. Laver, D. R. 2007. Ca^{2+} stores regulate ryanodine receptor Ca^{2+} release channels via luminal and cytosolic Ca^{2+} sites. *Biophys. J.* 92:3541–3555.
4. Laver, D. R., and B. N. Honen. 2008. Luminal Mg^{2+}, a key factor controlling RYR2-mediated Ca^{2+} release: cytoplasmic and luminal regulation modeled in a tetrameric channel. *J. Gen. Physiol.* 132:429–446.
5. Sitsapesan, R., and A. J. Williams. 1994. Gating of the native and purified cardiac SR Ca^{2+}-release channel with monovalent cations as permeant species. *Biophys. J.* 67:1484–1494.
6. Stern, M. D. 1992. Buffering of calcium in the vicinity of a channel pore. *Cell Calcium.* 13:183–192.
7. Zahradníková, A., and I. Zahradník. 1995. Description of modal gating of the cardiac calcium release channel in planar lipid membranes. *Biophys. J.* 69:1780–1788.
8. Zahradníková, A., M. Dura, and S. Györke. 1999. Modal gating transitions in cardiac ryanodine receptors during increases of Ca^{2+} concentration produced by photolysis of caged Ca^{2+}. *Pflugers Arch.* 438:283–288.
9. Saftenku, E., A. J. Williams, and R. Sitsapesan. 2001. Markovian models of low and high activity levels of cardiac ryanodine receptors. *Biophys. J.* 80:2727–2741.

10. Rosales, R. A., M. Fill, and A. L. Escobar. 2004. Calcium regulation of single ryanodine receptor channel gating analyzed using HMM/MCMC statistical methods. *J. Gen. Physiol.* 123:533–553.

11. Chen, H., G. Valle, …, P. Volpe. 2013. Mechanism of calsequestrin regulation of single cardiac ryanodine receptor in normal and pathological conditions. *J. Gen. Physiol.* 142:127–136.

12. Zhang, J., B. Chen, …, S. R. Chen. 2014. The cardiac ryanodine receptor luminal Ca^{2+} sensor governs Ca^{2+} waves, ventricular tachyarrhythmias and cardiac hypertrophy in calsequestrin-null mice. *Biochem. J.* 461:99–106.

13. Qin, J., G. Valle, …, M. Fill. 2008. Luminal Ca^{2+} regulation of single cardiac ryanodine receptors: insights provided by calsequestrin and its mutants. *J. Gen. Physiol.* 131:325–334.

14. Györke, I., N. Hester, …, S. Györke. 2004. The role of calsequestrin, triadin, and junctin in conferring cardiac ryanodine receptor responsiveness to luminal calcium. *Biophys. J.* 86:2121–2128.

15. Sigworth, F. J., and S. M. Sine. 1987. Data transformations for improved display and fitting of single-channel dwell time histograms. *Biophys. J.* 52:1047–1054.

16. Silverman, B. W. 1986. Density Estimation for Statistics and Data Analysis. Chapman & Hall, London, p. 176.

17. Boyce, W. E., and R. C. DiPrima. 1997. Elementary Differential Equations. John Wiley & Sons, New York.

18. Chamberlain, B. K., and S. Fleischer. 1988. Isolation of canine cardiac sarcoplasmic reticulum. *Methods Enzymol.* 157:91–99.

19. Tu, Q., P. Vélez, …, M. Fill. 1994. Streaming potentials reveal a short ryanodine-sensitive selectivity filter in cardiac Ca^{2+} release channel. *Biophys. J.* 67:2280–2285.

20. Beard, N. A., M. G. Casarotto, …, A. F. Dulhunty. 2005. Regulation of ryanodine receptors by calsequestrin: effect of high luminal Ca^{2+} and phosphorylation. *Biophys. J.* 88:3444–3454.

21. Gillespie, D. 2008. Energetics of divalent selectivity in a calcium channel: the ryanodine receptor case study. *Biophys. J.* 94:1169–1184.

22. Gaburjakova, J., and M. Gaburjakova. 2006. Comparison of the effects exerted by luminal Ca^{2+} on the sensitivity of the cardiac ryanodine receptor to caffeine and cytosolic Ca^{2+}. *J. Membr. Biol.* 212:17–28.

23. Szekely, G. J., M. L. Rizzo, and N. K. Bakirov. 2007. Measuring and testing dependence by correlation of distances. *Ann. Stat.* 35:2769–2794.

24. Szekely, G. J., and M. L. Rizzo. 2009. On Brownian distance covariance high dimensional data. *Ann. Appl. Stat.* 3:1266–1269.